A Numerical Self-Consistent Reaction Field (SCRF) Model for Ground and Excited States in NDDO-Based Methods

Guntram Rauhut,† Timothy Clark,*,† and Thomas Steinke‡

Contribution from the Institut für Organische Chemie der Friedrich-Alexander-Universität Erlangen-Nürnberg, Henkestrasse 42, D-91054 Erlangen, Germany, and Konrad-Zuse-Zentrum für Informationstechnik, Heilbronnerstrasse 10, D-10711 Berlin-Wilmersdorf, Germany

Received April 9, 1993®

Abstract: A numerical self-consistent reaction field (SCRF) technique for the calculation of solvent effects within the parametrized NDDO-based semiempirical molecular orbital methods has been developed and extended to excited states. The method uses Tomasi's treatment of the reaction field within an arbitrarily (van der Waals) shaped cavity. The dispersion contribution has been included via an oscillating dipole model. The model can treat both bathochromic and hypsochromic shifts for organic dyes successfully. Dispersion is found to be very important for some dyes, but to play almost no role for others.

Introduction

In the last three decades quantum chemistry has become a powerful tool for the investigation of organic molecules and chemical reactions in the gas phase. It is now a well-established and reliable method for predicting the electronic properties of organic molecules.[1] One disadvantage of many common SCF-based programs is that the wavefunction corresponds to the situation in a hypothetical motionless vacuum state, while most chemical reactions occur in solution. Therefore, much effort has been devoted in the last 15 years to the implementation of perturbations of the wave function of the molecule by a solvent. In this context the SCRF model,[2-4] which incorporates the reaction field directly into the Hamiltonian, has become popular for both *ab initio* and semiempirical molecular orbital treatments. Here we must distinguish between cavity models and those that do not need such a boundary between the solute and the solvent. We will consider the latter first.

One of the first steps toward a more realistic description of a chemical environment was introduced by the solvation model of Klopman,[5] Germer[6] and Miertuš,[7] based on the formalisms of Born.[8] In this approach the influence of the solvent on the solute is described by a discrete number of virtual charges, the solvatons. The solvaton charge is assumed to be equal to the negative of the net Mulliken[9] charge for the atomic center with which the solvation is associated. For one-center terms the solvation is placed at a van der Waals distance from the atom, while for two-center terms the solvaton is located at the center of the second atom.

Another model that requires no cavity surface was recently presented by Truhlar and co-workers.[10] They have included the solvent effect on the Hamiltonian by a strongly parametrized SCRF approach. This much more empirical model gives surprisingly good results, but it is limited to aqueous solution and is specific to either AM1[11] or PM3.[12] Warshel and Luzhkov[13] established two microscopic formalisms: the Langevin dipoles (LD)[14] and the surface constrained all atom solvent (SCAAS)[15] models within the MNDO[16] framework. Within the SCAAS/MNDO model each atom belonging to the solvent molecules is represented by a force-field-derived electrostatic potential that is included in the Hamiltonian explicitly. The model involves spherical boundary conditions that constrain the molecules on the surface. The LD ansatz described the interaction between the solute and the solvent by polarizable point dipoles in the first solvation sphere of the solute and a continuum outside this region.

A simplification of the LD two-sphere model above is an approach using only the polarizable continuum to represent the solvent. This is the group of cavity models. These approaches have the advantage of very short computation times compared to a supermolecule ansatz, especially if analytical definitions of the cavity are used. One disadvantage of these analytical approaches is that they are limited to spherical or ellipsoidal cavities in order that the interaction integrals can be evaluated analytically. In this manner Rivail and Rinaldi[17] established a formalism for semiempirical MO theory that represents the interaction integral by a complete one-center multipole expansion.

† Institut für Organische Chemie der Friedrich-Alexander-Universität Erlangen-Nürnberg.

‡ Konrad-Zuse-Zentrum für Informationstechnik.

• Abstract published in *Advance ACS Abstracts,* September 1, 1993.

(1) Hehre, W.; Radom, L.; Schleyer, P. v. R.; Pople, J. A. *Ab Initio Molecular Orbital Theory*; Wiley: New York, 1986.

(2) (a) Huron, M.-J.; Claverie, P. *J. Phys. Chem.* **1972**, *76*, 2123. (b) Huron, M.-J.; Claverie, P. *J. Phys. Chem.* **1974**, *78*, 1853, 1862.

(3) (a) Gómez-Jeria, J. S.; Conteras, R. R. *Int. J. Quantum Chem.* **1986**, *15*, 591. (b) Gómez-Jeria, J. S.; Morales-Lagos, D. *J. Phys. Chem.* **1990**, *94*, 3790. (c) Morales-Lagos, D.; Gómez-Jeria, J. S. *J. Phys. Chem.* **1991**, *95*, 5308.

(4) (a) Fox, T.; Rösch, N.; Zauhar, R. J. *J. Comput. Chem.* **1993**, *14*, 253. (b) Fox, T.; Rösch, N. *Chem. Phys. Lett.* **1992**, *191*, 33. (c) Zauhar, R. J.; Morgan, R. S. *J. Comput. Chem.* **1988**, *9*, 171.

(5) (a) Klopman, G. *Chem. Phys. Lett.* **1967**, *1*, 200. (b) Klopman, G.; Andreozzi, P. *Theor. Chim. Acta* **1980**, *55*, 77.

(6) (a) Germer, H. A. *Theor. Chim. Acta* **1974**, *34*, 145. (b) Germer, H. A. *Theor. Chim. Acta* **1974**, *35*, 273.

(7) (a) Miertuš, S.; Kysel, O. *Chem. Phys.* **1977**, 21, 27, 33, 47. (b) Duben, A. J.; Miertuš, S. *Theor. Chim. Acta* **1981**, *60*, 327.

(8) Born, M. *Z. Phys.* **1920**, *1*, 45.

(9) Mulliken, R. S. *J. Chem. Phys.* **1955**, *23*, 1833.

(10) (a) Cramer, C. J.; Truhlar, D. G. *J. Am. Chem. Soc.* **1991**, *113*, 8305. (b) Cramer, C. J.; Truhlar, D. G. *J. Am. Chem. Soc.* **1991**, *113*, 8552. (c) Cramer, C. J.; Truhlar, D. G. *Science* **1992**, *256*, 213. (d) Cramer, C. J.; Truhlar, D. G. *J. Comput. Chem.* **1992**, *13*, 1089.

(11) Dewar, M. J. S.; Zoebisch, E. G.; Healy, E. F.; Stewart, J. J. P. *J. Am. Chem. Soc.* **1985**, *107*, 3902.

(12) Stewart, J. J. P. *J. Comput. Chem.* **1989**, *10*, 209, 221.

(13) (a) Warshel, A. *Chem. Phys. Lett.* **1978**, *55*, 454. (b) Warshel, A. *J. Phys. Chem.* **1979**, *83*, 1640. (c) Luzhkov, V.; Warshel, A. *J. Am. Chem. Soc.* **1991**, *113*, 4491. (d) Luzhkov, V.; Warshel, A. *J. Comput. Chem.* **1992**, *13*, 199.

(14) Russel, S. T.; Warshel, A. *J. Mol. Biol.* **1985**, *185*, 389.

(15) King, G.; Warshel, A. *J. Chem. Phys.* **1989**, *91*, 3647.

(16) Dewar, M. J. S.; Thiel, W. *J. Am. Chem. Soc.* **1977**, *99*, 4899.

(17) (a) Rinaldi, D.; Rivail, J.-L. *Theor. Chim. Acta* **1973**, *32*, 57. (b) Rinaldi, D.; Rivail, J.-L. *Theor. Chim. Acta* **1974**, *32*, 243. (c) Rivail, J.-L.; Terryn, B. *J. Chem. Phys.* **1982**, *79*, 1. (d) Costa Cabral, B. J.; Rinaldi, D.; Rivail, J.-L. *Chem. Phys. Lett.* **1982**, *93*, 157. (e) Rinaldi, D.; Ruiz-Lopez, M. F.; Rivail, J.-L. *J. Chem. Phys.* **1983**, *78*, 834. (f) Ranaldi, D.; Ruiz-Lopez, M. F.; Rivail, J.-L. *J. Chem. Phys.* **1984**, *81*, 296. (g) Rivail, J.-L.; Terryn, B.; Rinaldi, D.; Ruiz-Lopez, M. F. *J. Mol. Struct. (THEOCHEM)* **1985**, *120*, 387. (h) Sánchez Marcos, E.; Pappalardo, R. P.; Rinaldi, D. *J. Phys. Chem.* **1991**, *95*, 8928. (i) Rinaldi, D.; Rivail, J.-L., Rguini, N. *J. Comput. Chem.* **1992**, *13*, 675.

0002-7863/93/1515-9174$04.00/0

Parallel to this work Christoffersen[18] developed the same method for *ab initio* MO theory. Mikkelsen[19] extended this approach to MCSCF wave functions. As well as the electrostatic contribution to the total energy of solvation usually considered, Rivail and Rinaldi also take the dispersion contribution into account. Tapia has also developed a method based on an analytical description of the cavity, but which is limited to the dipole contribution to the reaction field. While Karelson and Zerner[21] use this approach with different semiempirical Hamiltonians, Wiberg and co-workers[22] applied this ansatz to *ab initio* MO theory. The truncation of the multipole expansion beyond the dipole term seems to us somewhat critical because nonpolar molecules cannot be described properly without inclusion of higher multipole moments. The general disadvantage of all these analytical cavity models is that they are limited to molecules that are almost spherical or ellipsoidal. Especially the calculation of T or irregularly shaped molecules (e.g. enzymes) leads to significant problems. A spherical or ellipsoidal cavity also cannot represent the conformational changes in a molecular structure properly, e.g. the investigation of rotational barriers in solution is strongly limited because the reaction field acts too unspecifically on critical molecular fragments.

Therefore, continuum models that use an arbitrarily shaped boundary seem more promising for predicting solvent effects. This method was introduced by Tomasi[23] and Olivares del Valle[24] for *ab initio* formalisms. Ford,[25] Rösch,[4] and Basilevsky[26] used the same approach within semiempirical MO theory, while Sakurai[27] extended the method to an inhomogeneous dielectrics model. The arbitrarily shaped cavity in these models is defined by a finite set of surface elements, obtained from a fragmentation of the molecular surface constructed by interlocking spheres. For homogeneous dielectrics the perturbation of the Hamiltonian is given by the reaction field created by virtual charges placed on the finite surface elements. Details of this method will be given below.

The numerical description of the cavity surface prevents an analytical calculation of the interaction integrals, in contrast to the spherical or ellipsoidal cavity models mentioned above. This leads to time-consuming steps such as the calculation of electrostatic potentials and field strengths when determining the reaction field. Because of the advantages outlined above, however, we have implemented the arbitrarily shaped cavity model in our semiempirical MO program package.[28] In an extension compared to most approaches described in the literature, we have also considered the dispersion contribution (ΔG^{solv}_{disp}) and the contribution of the free cavity energy (ΔG^{solv}_{cav}). In this way the total free energy of solvation (ΔG^{solv}_{tot}) in our approach is given by

$$\Delta G^{solv}_{tot} = \Delta G^{solv}_{estat} + \Delta G^{solv}_{disp} + \Delta G^{solv}_{cav} \quad (1)$$

where ΔG^{solv}_{estat} is the electrostatic part of the free solvation energy. These additional components can cause large effects, as we will show in the applications below. We have also extended our methodology to excited states. Ruiz-Lopez *et al.*[29] used the random phase approximation to treat solvent effects in electronic spectra and both Zerner[21] and Rösch[4] have more recently used SCRF theory for excited states.

Theory

All calculations used the VAMP program,[28] which is input-compatible with MOPAC[30] and AMPAC.[31] Standard AM1 theory[11] was used throughout. Note that Thiel[32] has pointed out that standard MNDO (and AM1) theory does not give exactly rotationally invariant excited states. We expect these effects to be small in our case and have used the standard methodology throughout.

A. The Cavity. The algorithms of Pascual-Ahuir[33] and Connolly[34] are both suitable for defining an arbitrarily shaped cavity, but we have modified the approach of Marsili[35] using a marching-cube algorithm to obtain surface points. These points are connected by a subsequent next-neighbor algorithm to determine the surface area of each element and the corresponding normal vector. We have obtained an optimum with regard to computation time and accuracy of the electrostatic energy using a resolution of 0.216 au^3 for the volume of the marching cube. It is well-known that the surface of an arbitrarily shaped cavity needs many more planar surface patterns than curved ones to describe the surface and the potential at the surface correctly.[4a] Therefore, we have introduced two corrections to our flat patterns. Firstly, the electrostatic potential is not calculated in the center of the surface element, but at a corresponding point corrected to the van der Waals surface of the atom. Secondly, to correct the

(18) (a) Hylton, J.; Christoffersen, R. E.; Hall, G. G. *Chem. Phys. Lett.* **1974**, *26*, 501. (b) Hylton, McCreery, J.; Christoffersen, R. E.; Hall, G. G. *J. Am. Chem. Soc.* **1976**, *98*, 7191. (c) Burch, J. L.; Raghuveer, K. S.; Cristoffersen, R. E. In *Environmental Effects on Molecular Structure and Properties*; Pullman, B., Ed.; Reidel: Dordrecht, 1976; p 17.

(19) (a) Mikkelsen, K. V.; Dalgaard, E.; Swanstrøm, P. *J. Phys. Chem.* **1987**, *91*, 3081. (b) Mikkelsen, K. V.; Ratner, M. A. *Int. J. Quantum Chem. Symp.* **1987**, *21*, 341. (c) Mikkelsen, K. V.; Agren, H.; Jensen, H. J. A.; Helgaker, T. *J. Chem. Phys.* **1988**, *89*, 3086. (d) Medina-Llanos, C.; Agren, H.; Mikkelsen, K. V.; Jensen, H. J. A. *J. Chem. Phys.* **1989**, *90*, 6422. (e) Agren, H.; Mikkelsen, K. V. *J. Mol. Struct. (Theochem)* **1991**, *234*, 425.

(20) (a) Tapia, O.; Goscinski, O. *Mol. Phys.* **1975**, *29*, 1653. (b) Tapia, O. *Theor. Chim. Acta* **1978**, *47*, 157. (c) Constanciel, R.; Tapia, O. *Theor. Chim. Acta* **1978**, *48*, 75. (d) Tapia, O.; Silvi, B. *J. Phys. Chem.* **1980**, *84*, 2646. (e) Tapia, O. In *Quantum Theory of Chemical Reactions*; Daudel, R., Pullman, A., Salem, L., Veillard, A., Eds.; Reidel: Dordrecht, 1980; Vol. 2, p 25. (f) Tapia, O. In *Molecular Interactions*; Orville-Thomas, W. J., Ed.; Wiley: New York, 1982; Vol. 3, Chaper 2. (g) Tapia, O. In *Theoretical Models of Chemical Bonding*; Maksić, Z. B., Ed.; Springer: Berlin, Heidelberg, 1991; Vol. 4, p 435. (h) Tapia, O. *J. Mol. Struct. (Theochem.)* **1991**, *226*, 59.

(21) (a) Karelson, M. M.; Tamm, T.; Katritzky, A. R.; Cato, S. J.; Zerner, M. C. *Tetrahedron Comput. Methodol.* **1989**, *2*, 295. (b) Karelson, M. M.; Katritzky, A. R.; Szafran, M.; Zerner, M. C. *J. Org. Chem.* **1989**, *54*, 6030. (c) Rzepa, H. S.; Yi, M. Y.; Karelson, M. M.; Zerner, M. C. *J. Chem. Soc., Perkin Trans. 2* **1991**, 635. (d) Katritzky, A. R.; Karelson, M. M. *J. Am. Chem. Soc.* **1991**, *113*, 1561. (e) Karelson, M. M.; Zerner, M. C. *J. Phys. Chem.* **1992**, *96*, 6949.

(22) (a) Wong, M. W.; Frisch, M. J.; Wiberg, K. B. *J. Am. Chem. Soc.* **1991**, *113*, 4776. (b) Wong, M. W.; Wiberg, K. B.; Frisch, M. J. *J. Am. Chem. Soc.* **1992**, *114*, 523. (c) Wong, M. W.; Wiberg, K. B.; Frisch, M. J. *J. Am. Chem. Soc.* **1992**, *114*, 1645.

(23) (a) Miertuš, S.; Scrocco, E.; Tomasi, J. *Chem. Phys.* **1981**, *55*, 117. (b) Miertuš, S.; Tomasi, J. *Chem. Phys.* **1982**, *65*, 239. (c) Bonaccorsi, R.; Cimiraglia, R.; Tomasi, J. *J. Comput. Chem.* **1983**, *4*, 567. (d) Tomasi, J.; Alagona, G.; Bonaccorsi, R.; Ghio, G. In *Modelling of Structure and Properties of Molecules*; Maksić, Z. B., Ed.; Wiley: New York, 1987; p 330. (e) Floris, F.; Tomasi, J. *J. Comput. Chem.* **1989**, *10*, 616. (f) Bonaccorsi, R.; Cammi, R.; Tomasi, J. *J. Comput. Chem.* **1991**, *12*, 301. (g) Tomasi, J.; Bonaccorsi, R.; Cammi, R.; Olivares del Valle, F. J. *J. Mol. Struct. (THEOCHEM)* **1991**, *234*, 401. (h) Tuñón, I.; Silla, E.; Tomasi, J. *J. Phys. Chem.* **1992**, *96*, 9043.

(24) (a) Aguilar, M. A.; Olivares del Valle, F. J. *Chem. Phys.* **1989**, *129*, 439. (b) Aguilar, M. A.; Olivares del Valle, F. J. *Chem. Phys.* **1989**, *138*, 327. (c) Olivares del Valle, F. J.; Tomasi, J. *Chem. Phys.* **1991**, *150*, 139. (d) Aguilar, M. A.; Olivares del Valle, F. J.; Tomasi, J. *Chem. Phys.* **1991**, *150*, 151. (e) Tolosa, S.; Esperilla, J. J.; Olivares del Valle, F. J. *J. Comput. Chem.* **1990**, *11*, 576. (f) Cammi, R.; Olivares del Valle, F. J.; Tomasi, J. *Chem. Phys.* **1988**, *122*, 63. (g) Olivares del Valle, F. J.; Aguilar, M. A. *J. Comput. Chem.* **1992**, *13*, 115.

(25) (a) Ford, G. P.; Wang, B. *J. Comput. Chem.* **1992**, *13*, 229. (b) Wang, B.; Ford, G. P. *J. Chem. Phys.* **1992**, *97*, 4162.

(26) Chudinov, G. E.; Napolov, D. V.; Basilevsky, M. V. *Chem. Phys.* **1991**, *160*, 41.

(27) Hoshi, H.; Sakurai, M.; Inoue, Y.; Chûjô, R. *J. Chem. Phys.* **1987**, *87*, 1107.

(28) Rauhut, G.; Alex, A.; Chandrasekhar, J.; Clark, T. *VAMP 4.5*, Oxford Molecular Ltd., Oxford, 1993.

(29) (a) Ruiz-Lopez, M. F.; Rinaldi, D. *J. Mol. Struct. (THEOCHEM)* **1983**, *93*, 277. (b) Ruiz-Lopez, M. F.; Rinaldi, D. *Chem. Phys.* **1984**, *86*, 367. (c) Ruiz-Lopez, M. F.; Rinaldi, D.; Rivail, J.-L. Chem. *Phys.* **1986**, *110*, 403.

(30) MOPAC, Version 4.0, QCPE, Program No. 455.

(31) AMPAC, Version 1.0, QCPE, Program No. 506.

(32) Thiel, W.; Voityuk, A. A. *Theor. Chim. Acta* **1992**, *81*, 391.

(33) (a) Pascual-Ahuir, J. L.; Silla, E.; Tomasi, J.; Bonaccorsi, R. *J. Comput. Chem.* **1987**, *8*, 778. (b) Pascual-Ahuir, J. L.; Silla, E. *J. Comput. Chem.* **1990**, *11*, 1047. (c) Silla, E.; Tuñón, I.; Pascual-Ahuir, J. L. *J. Comput. Chem.* **1991**, *12*, 1077.

(34) (a) Connolly, M. L. *J. Appl. Crystallogr.* **1983**, *16*, 548. (b) Connolly, M. L. *Molecular Surface Program*, QCPE No. 429.

(35) Marsili, M. In *Physical Property Prediction in Organic Chemisty*; Jochum, C., Hicks, M. G., Sunkel, J., Eds.; Springer: Berlin, 1988; p 249.

planar surface elements (Δs_s^0) themselves to the convex shape of the molecular surface we have introduced a scaling function of the form

$$\Delta s_s = \Delta s_s^0(1 + aD^2) \tag{2}$$

D is the distance between the center of the surface element and the molecular surface along the normal vector and a is an empirically derived parameter found to be 0.2 au^{-2}. These corrections lead to faster convergence in the total surface area and the total energy of solvation when the number of surface patterns is increased. The results relative to surface characteristics and the electrostatic energy obtained by using this method are comparable with those using the method of Connolly or Pascual-Ahuir.

The free cavity energy was calculated by following the approaches suggested by Pierotti[36] and therefore depends only on the total surface area and the solute's diameter and volume.

B. The Molecular Electrostatic Potential and Its Gradient. Within SCRF theory using numerically derived cavities the molecular electrostatic potential (MEP) determines the quality of the reaction field and the electrostatic interaction free energy (ΔG_{estat}^{solv}) shown below.

$$\Delta G_{estat}^{solv} = (E_{tot}^{solv} - E_{tot}^{vac}) - {}^1/_2\sum_s q_s V(\vec{r}_s) \tag{3}$$

Where q_s is the virtual charge of the surface element s, and $V(\vec{r}_s)$ is the molecular electrostatic potential at the center $\vec{r}_s$ of this surface element. The polarization of the molecule by the solvent leads to the term involving the difference between the vacuum total energy (E_{tot}^{vac}) and that in the reaction field (E_{tot}^{solv}). The large number of surface elements and the calculation of the reaction field in each SCRF cycle require very fast computation of the MEP. Recently, we introduced the NAO/PC model for calculating molecular electrostatic potentials.[37] This method, which is similar to the distributed multipole approach,[38] fulfills both requirements. Our calculation of the MEP is about 1000 times faster than the algorithm used in MOPAC-ESP[39] and shows lower root-mean-square errors compared to a potential calculated at RHF/6-31G*.[40] In this approach the integral over the electronic charge distribution in the definition of the MEP ($V(\vec{r})$)

$$V(\vec{r}) = \sum_\alpha \frac{Z_\alpha}{|\vec{R}_\alpha - \vec{r}|} - \int \frac{\rho(\vec{r}')\,d\vec{r}'}{|\vec{r}' - \vec{r}|} \tag{4}$$

is replaced by a summation over the point charges derived from the NAOs.[41]

$$\int \frac{\rho(\vec{r}')\,d\vec{r}'}{|\vec{r}' - \vec{r}|} \approx -\sum_{\alpha(\alpha\notin H)} \sum_{i=1}^{2n_\alpha^{orb}} \frac{q_{i\alpha}}{|\vec{r}_{i\alpha} - \vec{r}|} - \sum_{\alpha(\alpha\in H)} \frac{q_\alpha}{|\vec{R}_\alpha - \vec{r}|} \tag{5}$$

In these formulae Z_α is the core charge of atom α at the position $\vec{R}_\alpha$. $\rho(\vec{r})$ is the electronic charge density and $q_{i\alpha}$ is the ith NAO point charge of the $2n_\alpha^{orb}$ point charges of atom α at the position $\vec{r}_{i\alpha}$. n_α^{orb} is the number of basis functions on atom α. The first sum on the right-hand side of formula 5 loops over all non-hydrogen atoms, while the sum in the second term loops over all hydrogens. The gradient of the molecular electrostatic potential (see eq 4), which will be required later, can also be calculated easily within the NAO/PC model (eq 5):

$$\vec{E}(\vec{r}) = -\frac{\partial V(\vec{r})}{\partial \vec{r}} = -\sum_\alpha \frac{Z_\alpha(\vec{R}_\alpha - \vec{r})}{|\vec{R}_\alpha - \vec{r}|^3} - \sum_{\alpha(\alpha\notin H)} \sum_{i=1}^{2n_\alpha^{orb}} \frac{q_{i\alpha}(\vec{r}_{i\alpha} - \vec{r})}{|\vec{r}_{i\alpha} - \vec{r}|^3} - \sum_{\alpha(\alpha\in H)} \frac{q_\alpha(\vec{R}_\alpha - \vec{r})}{|\vec{R}_\alpha - \vec{r}|^3} \tag{6}$$

Here $\vec{E}(\vec{r})$ is the corresponding electric field. The calculation of the NAO point charges and their positions has been described in detail elsewhere.[37]

C. The Reaction Field. The reaction field is an electrostatic field that results from the polarization of the (usually homogeneous) dielectric continuum by a charge distribution inside the cavity. The dependence of the reaction field strength on macroscopic quantities, usually the dielectric constant (ϵ) and the refraction index, can be described by a variety of functions $f(\epsilon(\omega))$.[42] They differ in how the orientational and electronic components of the polarization of the solvent are included in the simulation. We have used the ansatz of Born,[8] Kirkwood,[43] and Onsager.[44]

$$f(\epsilon(0)) = \frac{\epsilon(0) - 1}{4\pi} \tag{7}$$

The function $f(\epsilon(\omega))$ describes the geometrical relaxation of the solvent molecules dependent on the frequency (ω). Usually two critical cases are considered: firstly, infinitely fast relaxation that corresponds to $\epsilon(0)$, secondly, infinitely slow relaxation that corresponds to $\epsilon(\infty) = n^2$, where n is the refractive index.

Following the suggestions of Tomasi[23a] the induced surface charge density at the position $\vec{r}_s$ ($\sigma(\vec{r}_s)$) is given by

$$\sigma(\vec{r}_s) = -f(\epsilon(\omega))\,\vec{E}(\vec{r}_s)\cdot\vec{n}_s \tag{8}$$

where $\vec{n}_s$ is the normal vector of a given surface point directed toward the dielectric. Besides this commonly used approach we have also implemented the algorithms for considering self-polarization in calculating the surface charges.[23] Starting from eq 8 and a subsequent discretization one obtains

$$q_{s\alpha}^m = q_{s\alpha}^0 - f(\epsilon(\omega))\frac{\Delta s_{s\alpha}}{\epsilon(\omega)|\delta\vec{n}_{s\alpha}|}\sum_{s\neq t} q_{t\beta}^{m-1}\left(\frac{1}{|\vec{r}_{s\alpha} + \delta\vec{n}_{s\alpha} - \vec{r}_{t\beta}|} - \frac{1}{|\vec{r}_{s\alpha} - \vec{r}_{t\beta}|}\right) + f(\epsilon(\omega))\frac{2\pi}{\epsilon(\omega)}q_{s\alpha}^{m-1}\left(1 - \sqrt{\frac{\Delta s_{s\alpha}}{4\pi R_{s\alpha}{}^2}}\right) \tag{9}$$

$q_{s\alpha}$ is the sth surface charge on atom α, δ is an infinitesimal distance (we have used a value of 0.01 a.u. in our calculations throughout) and $R_{s\alpha}$ is the distance of the surface element to the center of its sphere (atom). m is the counter for the self-polarization cycles.

The tail of the solute's wave function lying outside the cavity leads to a total surface charge that is not equal and opposite in sign to the total charge of the solute. Therefore, we have used the method of charge compensation proposed by Tomasi and co-workers.[23a]

$$\tilde{q}_s^{\pm} = q_s^{\pm}(1 - \sum_s q_s/2\sum_{s\in\pm} q_s^{\pm}) \tag{10}$$

where $q_s^{\pm}$ are the positive or negative charge elements, respectively.

(36) (a) Pierotti, R. A. *J. Phys. Chem.* **1963**, *67*, 1840. (b) Pierotti, R. A. *Chem. Rev.* **1976**, *76*, 717.
(37) Rauhut, G.; Clark, T. *J. Comput. Chem.* **1993**, *14*, 503.
(38) (a) Stone, A. J. *Chem. Phys. Lett.* **1981**, *83*, 233. (b) Fowler, P. W. *J. Phys. Chem.* **1987**, *91*, 509. (c) Stone, A. J.; Price, S. L. *J. Phys. Chem.* **1988**, *92*, 3325. (d) Stone, A. J. In *Theoretical Models of Chemical Bonding*; Maksić, Z. B., Ed.; Springer: Berlin, 1991; Vol. 4, p 103.
(39) (a) Merz, K. M.; Besler, B. H. *MOPAC-ESP*, QCPE No. 589. (b) Merz, K. M.; Besler, B. H. MOPAC-ESP In *QCPE Bull.* **1990**, *10*, 15.
(40) (a) Hariharan, P. C.; Pople, J. A. *Theor. Chim. Acta* **1973**, *28*, 213. (b) Francl, M. M.; Pietro, W. J.; Hehre, W. J.; Binkley, J. S.; Pople, J. A. *J. Chem. Phys.* **1982**, *77*, 3654.
(41) Foster, J. P.; Weinhold, F. *J. Am. Chem. Soc.* **1980**, *102*, 7211.
(42) Kolling, O. W. *J. Phys. Chem.* **1991**, *95*, 3950.
(43) (a) Kirkwood, J. G. *J. Chem. Phys.* **1934**, *2*, 351. (b) Kirkwood, J. G.; Westheimer, F. H. *J. Chem. Phys.* **1938**, *6*, 506.
(44) Onsager, L. *J. Am. Chem. Soc.* **1936**, *58*, 1486.

D. The Perturbation of the Hamiltonian. Within self-consistent reaction field theory the influence of the solvent on the electronic properties of the solute is treated quantum mechanically by an additional one-electron term to the Hamiltonian of the solute *in vacuo*.

$$\hat{H} = \hat{H}^0 - \sum_s \sum_i \frac{q_s}{r_{si}} + \sum_s \sum_\alpha \frac{q_s Z_\alpha}{r_{s\alpha}} \tag{11}$$

while r_{si} is the distance between the ith electron and the sth surface element, $r_{s\alpha}$ is the distance between the αth core and the considered surface element. The new Fock operator ($\hat{f}(i)$) is thus given by

$$\hat{f}(i) = \hat{f}^0(i) - \sum_s \frac{q_s}{r_{si}} \tag{12}$$

Considering the corresponding matrix **F** in the basis of atomic orbitals the additional term is given by

$$F_{\mu\nu} = F^0_{\mu\nu} - \sum_s q_s \left\langle \mu \left| \frac{1}{r_{si}} \right| \nu \right\rangle \tag{13}$$

As usually used in the NDDO approximation,[45] these one-electron integrals are substituted by the corresponding two-electron integral.

$$\left\langle \mu^{(\alpha)} \left| \frac{1}{r_{si}} \right| \nu^{(\beta)} \right\rangle \approx \langle \mu^{(\alpha)} \nu^{(\beta)} | s^s s^s \rangle \delta_{\alpha\beta} \tag{14}$$

Dewar and Thiel[46] have approximated the two-electron integrals by a parametrized multipole expansion in the framework of MNDO-based methods. We have modified this approach because one center of this integral is not a charge distribution but a point charge. Therefore, we have omitted all integral parameters corresponding to the point charge. This leads to the following two-center integrals:

$$\langle s^\alpha s^\alpha | s^s s^s \rangle \approx \frac{1}{\sqrt{R_{\alpha s}^{\,2} + (2A_{M\alpha})^{-2}}} \tag{15}$$

$$\langle s^\alpha p^\alpha | s^s s^s \rangle \approx \frac{1}{2\sqrt{(R_{\alpha s} + D_{1\alpha})^2 + (2A_{D\alpha})^{-2}}} - \frac{1}{2\sqrt{(R_{\alpha s} - D_{1\alpha})^2 + (2A_{D\alpha})^{-2}}} \tag{16}$$

$$\langle p^\alpha_\sigma p^\alpha_\sigma | s^s s^s \rangle \approx \langle s^\alpha s^\alpha | s^s s^s \rangle + \frac{1}{4\sqrt{(R_{\alpha s} + 2D_{2\alpha})^2 + (2A_{Q\alpha})^{-2}}} - \frac{1}{2\sqrt{R_{\alpha s}^{\,2} + (2A_{Q\alpha})^{-2}}} + \frac{1}{4\sqrt{(R_{\alpha s} - 2D_{2\alpha})^2 + (2A_{Q\alpha})^{-2}}} \tag{17}$$

$$\langle p^\alpha_\pi p^\alpha_\pi | s^s s^s \rangle \approx \langle s^\alpha s^\alpha | s^s s^s \rangle + \frac{1}{2\sqrt{R_{\alpha s}^{\,2} + 4D_{2\alpha}^{\,2} + (2A_{Q\alpha})^{-2}}} - \frac{1}{2\sqrt{\sqrt{R_{\alpha s}^{\,2}} + (2A_{Q\alpha})^{-2}}} \tag{18}$$

$A_{M\alpha}$, $A_{D\alpha}$, and $A_{Q\alpha}$ are parameters corresponding to the monopole, dipole, and quadrupole distribution of the electronic charge which result from the semiempirical parametrization.[47] $D_{1\alpha}$ and $D_{2\alpha}$ are constants related to the Slater exponents of the orbitals at atom α and the principal quantum number. This approach is different to that reported by Ford,[25b] who neglected the parameters $A_{X\alpha}$ and $D_{N\alpha}$, but whose implementation corresponds to a perturbation at the CNDO level. Basilevsky[26] also omitted the $D_{N\alpha}$ constants in eqs 15–18. Both authors reported difficulties related to charge conservation on the cavity surface resulting from the tails of the wave function outside the cavity. We found no such problems because we used the charge compensation procedure described above and possibly because of the calculation of the molecular electrostatic field by the NAO/PC model. In this way the one-center terms of the Fock matrix can be calculated by

$$F_{\mu\alpha\nu\alpha} = F^0_{\mu\alpha\nu\alpha} - \sum_s q_s \langle \mu^\alpha \nu^\alpha | s^s s^s \rangle \tag{19}$$

E. The Dispersion Contribution. When both large nonpolar solutes and solvent molecules are treated, the contribution of the dispersion energy to the total solvation interaction is very solvent specific and can be larger than the pure electrostatic interaction. Atom pair dispersion potentials from classical empirical C_6 coefficients are usually used to include this dispersion effect in the solvent simulation.[23e] This approach based on two-center potentials has the disadvantage that state-dependent dispersion effects cannot be taken into account. Therefore, we have used the approach of Olivares del Valle[24b] based on the ideas of Linder[48] treating the dispersion interaction of the solute with the continuum by a term related to the molecular polarizability:

$$\Delta G^{\text{solv}}_{\text{disp}} = -\frac{1}{8} \frac{\text{IP}_\text{m}\text{IP}_\text{s}}{\text{IP}_\text{M} + \text{IP}_\text{S}} \sum_l \sum_k \alpha_{lk} g_{lk}(\epsilon(\infty)) \tag{20}$$

IP_M and IP_S are the first ionization potential of the solute and the solvent, respectively. $\overleftrightarrow{\alpha}$ is the molecular polarizability tensor and $\overleftrightarrow{g}$ the reaction field tensor defined below. This equation combines the second-order response quantity ($\overleftrightarrow{\alpha}$) with a quantity describing the generated reaction field. The ionization potentials used in eq 20 have the function of weight factors.[49] Note that this has been discussed extensively in the literature.[24b,48,49] The dispersion contribution as given by eq 20 is strongly state dependent because of the sensitivity of the molecular polarizability, which is directly dependent on the molecular wave function. The ionization potential should also be state dependent, but in the absence of an exactly defined quantity within our approach we have used the ground-state IP calculated according to Koopmans' theorem[50] for all states. We note that, because of the series of approximations used to obtain eq 20 and because of the almost arbitrary nature of the factor involving the ionization potentials, the calculation of the dispersion term is essentially semiempirical. There may well be room for considerable improvement in accuracy relative to experiment by using another form of weighting factor in eq 20.

The variational method suggested by Rinaldi and Rivali[17b] was used to obtain the polarizability tensor ($\overleftrightarrow{\alpha}$). Thus this tensor is given by

$$\overleftrightarrow{\alpha} = \frac{4}{n_{\text{el}}} \overleftrightarrow{Q}^2 \tag{21}$$

with

$$Q_{kl} = \sum_\mu \sum_\nu P_{\mu\nu} \left[\langle \mu | x_k x_l | \nu \rangle - \frac{1}{2} \sum_\lambda \sum_\rho P_{\lambda\rho} \langle \mu | x_k | \lambda \rangle \langle \nu | x_l | \rho \rangle \right] \tag{22}$$

P symbolizes the density matrix, while l and k describe the direction in the coordinate system. On the basis of the model of

(45) Pople, J. A.; Santry, D. P.; Segal, G. A. *J. Chem. Phys.* **1965**, *43*, S129.
(46) Dewar, M. J. S.; Thiel, W. *Theor. Chim. Acta* **1977**, *46*, 89.
(47) Stewart, J. J. P. *J. Comp.-Aided Mol. Des.* **1990**, *4*, 1.
(48) (a) Linder, B. *J. Chem. Phys.* **1960**, *33*, 668. (b) Linder, B. *J. Chem. Phys.* **1961**, *35*, 371. (c) Linder, B. *J. Chem. Phys.* **1962**, *37*, 963.
(49) London, F. *Trans. Faraday Soc.* **1937**, *33*, 8.
(50) Koopmans, T. *Physica* **1933**, *1*, 104.
(51) Peyerimhoff, S. D.; Buenker, R. J. *Theor. Chim. Acta* **1970**, *19*, 1.

fluctuating dipoles the reaction field tensor $\overleftrightarrow{g}$ can be determined assuming an unpolarizable dipole to describe the solute charge distribution.[24b] The $\overleftrightarrow{g}$ tensor is found to be

$$\overleftrightarrow{g} = -\sum_s \frac{\vec{C}(\vec{r}_s) \otimes \vec{r}_s}{|\vec{r}_s|^3} \tag{23}$$

where $\vec{C}(\vec{r}_s)$ results from the dipolar electrostatic field influenced by the continuum at the cavity surface $\vec{r}_s$. $\otimes$ symbolizes a tensor product. Our implementation calculates the $\vec{C}$ field including the self-polarization cycles and uses the center of mass as the origin for the **g** tensor. Equation 22 is valid only at the SCF level. Strictly speaking, for excited states we should also consider terms arising from the two-particle reduced density matrix in addition to those given in eq 22. We expect these terms to be small, however (but have not tested this assumption). Furthermore, considering the one-particle terms in eq 22 is consistent with our use of the corresponding density matrix for excited states (see below). The results appear to justify these approximations, but we plan to investigate their effect.

F. The SCRF Expansion to Excited States. The SCRF method presented here has also been extended to calculations including configuration interaction (CI). In this context the two cases of the relaxation model mentioned above must be considered: firstly, infinitely fast geometrical relaxation of the solvent molecules, and secondly, infinitely slow geometrical relaxation.

In the first case the reaction field is determined by $\epsilon(0)$ for all states in the CI expansion. We have used the first-order correlated density matrix[52] for calculating the electrostatic component of the total energy of solvation and for calculating the polarizability tensor within the dispersion contribution (see eq 20). In this way the electrostatic contribution to any state S is given by

$$E^{\text{solv}}_{\text{estat}}(S) = {}^1/_2 \sum_s \Delta s_s f(\epsilon(0)) \vec{E}(\vec{r}_s,S)\cdot\vec{n}_s V(\vec{r}_s,S) \tag{24}$$

While this case refers to stable excited states with respect to the solvent reorientation, the second case is needed in considering electronic spectra. Tomasi[23] has expanded SCRF theory to absorption and emission transition, but we have implemented the method for absorption spectra only. Such a fast process leads to a new electronic charge distribution of the solute that changes the polarization of the solvent. Therefore, the polarization vector must be divided into an orientational and an electronic component:

$$\vec{P} = \vec{P}_{\text{or}} + \vec{P}_{\text{el}} \tag{25}$$

Hence it follows that the orientational part of the surface charge distribution is given by (see eq 8)

$$\sigma_{\text{or}} = [f(\epsilon(\infty)) - f(\epsilon(0))]\, \vec{E}(\vec{r}_s)\cdot\vec{n}_s \tag{26}$$

The orientational contribution of the ground state's (GS) surface charge distribution is equal for all states in the CI expansion. In contrast, the contribution that corresponds to the polarization of the solvent's electrons is state dependent. Therefore, the total surface charge distribution of an excited state (ES) is given by

$$\sigma(\text{ES}) = \sigma_{\text{or}}(\text{GS}) - f(\epsilon(\infty))\, \vec{E}(\vec{r}_s,\text{ES})\cdot\vec{n}_s \tag{27}$$

This splitting of the surface charge distribution has to be considered in the self-polarization cycles given by eq 9. Within these cycles ω is ∞ for excited states and the charges q must be replaced by the sum of the orientational and electronic components.[23]

The state-dependent polarizability tensor within the dispersion contribution is independent of the dielectric constant, but rather dependent on the correlated density matrix $P_{\mu\nu}$ only. It can therefore be used without change. The weighting factor expressed by the ionization potentials in the dispersion contribution in this approach is the most difficult. The ionization potential must also be state dependent, but we know of no suitable semiempirical method for calculating such potentials. Therefore, we have used Koopmans' theorem of ionization potential of the ground state and have damped the dispersion contribution to excited states by an empirical factor of 13%. This correction includes the error of about 10% by the ionization potential calculated via Koopmans' theorem.[51] It also includes the state dependence of the weighting factor. This approximation is clearly not very satisfactory, but it works rather well for the systems investigated and is consistent with the semiempirical nature of eq 20.

Table I. Physical Data Used for the Aprotic Solvents (Set 1)

solvent	$\epsilon_r(0)^a$	$\epsilon_r(\infty)^b$	IP[c] (au)
hexane	2.02	1.891	0.374
benzene	2.27	2.253	0.339
diethyl ether	4.20	1.828	0.353
chloroform	4.81	2.082	0.420
dichloromethane	8.93	2.028	0.417
pyridine	12.91	2.280	0.355
acetone	20.56	1.847	0.356
nitrobenzene	34.78	2.421	0.388
acetonitrile	35.94	1.806	0.448
dimethyl sulfoxide	46.45	2.184	0.331

[a] $\epsilon(0)$ = static dielectric constant. [b] $\epsilon(\infty)$ = dielectric constant at infinite frequency (n^2). [c] IP = first ionization potential.

Applications

The most obvious test of any SCRF theory is its ability to reproduce solvation free energies. We will, however, consider this aspect in a later paper and concentrate here on the calculation of solvatochromic shifts. Generally, our model performs better for solvation free energies than analytical SCRF methods, but not as well for calculations in water as Truhlar's parametrized procedure.[10] We have thus concentrated on properties that require configuration interaction.[52] In this context the calculation of solvent shifts in UV/vis spectra is one of the most attractive subjects. Miertuš and Kysel[7a] have investigated the solvent effect on electronic spectra of a series of radical anions at the CNDO/S level. At the same level Botrel et al.[53] have investigated the solvatochromism of benzophenone. Karelson and Zerner[21e] have recently calculated the solvent shifts of some more complex dyes. Using an SCRF approach that is much more comparable with our own, Fox and Rösch[4b] have used INDO/S to calculate the solvent shift of the $n \rightarrow \pi^*$ transition in acetone.

A. Methods. In the calculation of the UV/vis spectra we have used a CI expansion of 8 electrons in 9 MOs. Furthermore, we have limited the CI to single and pair double-excitations (PECI = 8) to give 49 configurations. This expansion gives reliable UV/vis spectra of most organic molecules.[54] The AM1-calculated gas-phase structure of the molecules was assumed for all calculations. We have considered two sets of solvents, shown in Tables I and II.[55] We have distinguished between protic (hydrogen bonding) and aprotic solvents. This distinction is useful because the representation of hydrogen bonding by continuum models is strongly limited. For the description of the cavity surface we have used the atomic van der Waals radii introduced by Bondi,[56] multiplied by a factor of 1.15 (Table III). This empirical factor, which is similar to Tomasi's factor of 1.2 for *ab initio* basis sets,[23a] corrects Bondi's radii to values that are usually used in force

(52) Armstrong, D. R.; Fortune, R.; Perkins, P. G.; Stewart, J. J. P. *J. Chem. Soc., Faraday Trans. 2* **1972**, *68*, 1839.

(53) Botrel, A.; Corre, F.; Le Beuze, A. *Chem. Phys.* **1983**, *74*, 383.

(54) (a) Clark, T.; Chandrasekhar, J. *Isr. J. Chem.*, in press. (b) Clark, T. presented at the NATO-ASI conference, Ponta Delgada (P), 1992.

(55) Physical data taken from refs 12, 60d, and the following: *Handbook of Chemistry and Physics*, 70th ed.; Weast, R. C., Ed.; CRC Press: Boca Raton, FL, 1989.

(56) Bondi, A. *J. Phys. Chem.* **1964**, *68*, 441.

Figure 1. Mesomeric structures of 4-[(4′-hydroxyphenyl)azo]-*N*-methylpyridine (**1**).

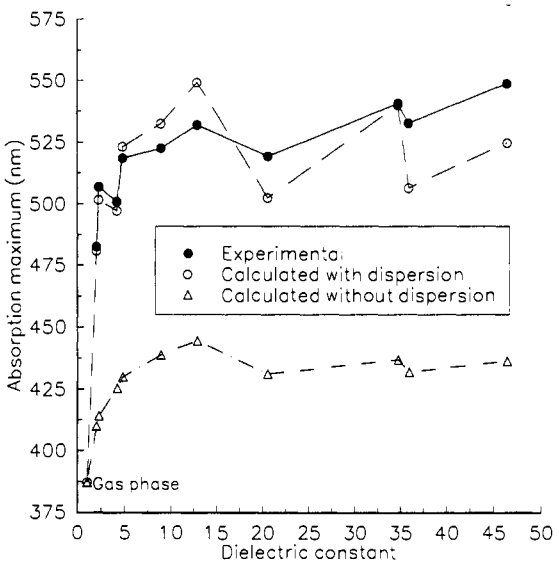

Figure 2. Solvent dependence of 4-[(4′-hydroxyphenyl)azo]-*N*-methylpyridine (**1**) for the case of infinitely slow solvent reorientation.

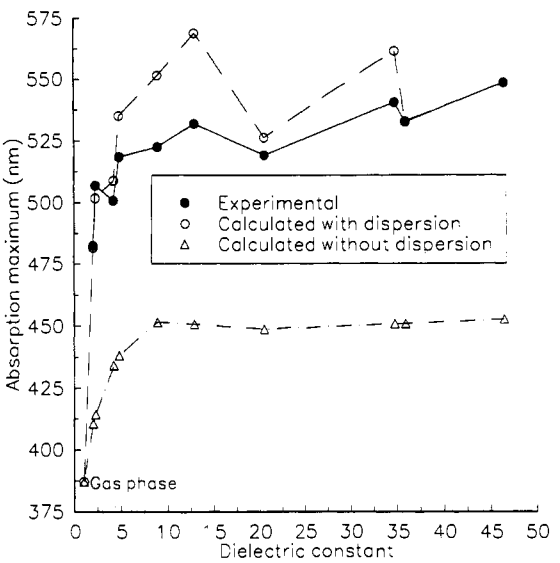

Figure 3. Solvent dependence of 4-[(4′-hydroxyphenyl)azo]-*N*-methylpyridine (**1**) in the case of infinitely fast solvent reorientation.

Table II. Physical Data Used for the Protic Solvents (Set 2)

solvent	$\epsilon_r(0)^a$	$\epsilon_r(\infty)^b$	IP[c] (au)
ethanol	24.55	1.852	0.386
methanol	32.66	1.764	0.398
water	78.36	1.777	0.463

[a] $\epsilon(0)$ = static dielectric constant. [b] $\epsilon(\infty)$ = dielectric constant at infinite frequency (n^2). [c] IP = first ionization potential.

Table III. Scaled van der Waals Radii for the Generation of the Cavity Surface

	H	C	N	O
radius (Å)	1.38	1.96	1.78	1.75

fields. In our calculations we have included self-polarization of the surfaces charges, using 4 cycles in both the iterations within the electrostatic and the dispersion contribution. The ionization potential was calculated by Koopmans' theorem as discussed above.[50]

We have calculated the spectra in two ways, firstly assuming infinitely slow relaxation of the solvent and secondly considering the case of infinitely fast relaxation. The contribution of the individual components (electrostatic, dispersion) will be considered below.

B. Bathochromic Solvent Shifts. We have investigated the solvatochromism of 4-[(4′-hydroxyphenyl)azo]-*N*-methylpyridine (**1**). This dye has been investigated extensively experimentally by Buncel.[57] He measured a strong bathochromic solvent shift in 29 different solvents. This strong shift is influenced by an intramolecular electron transfer that is initiated by the polarization through the solvent. The dye is thus presented by the two mesomeric structures shown in Figure 1.

Considering the case of infinitely slow relaxation of the solvent molecules for the solvatochromic band of Buncel's dye as a function of the solvent gives the results shown in Figure 2. In all figures presented here the solvent is represented by its dielectric constant. The agreement between the experimental data of Buncel and our calculated results is excellent for the aprotic solvents. The general trend of this curve as well as its fine structure are reproduced well. Furthermore, the dispersion contribution dominates the observed shifts in this example. At higher dielectric constants the solvent shifts are overestimated by about 10–20 nm. This may be a geometrical effect because the gas-phase structure underestimates the importance of the bond stretching in the left-hand mesomeric structure of **1** in Figure 1. This structure becomes more important in polar solvents. Consideration of the electrostatic component of the total solvation energy alone gives absorption maxima that are shifted by about 100 nm to lower wavelengths. The electrostatic component shows a comparable fine structure at higher dielectric constants, but fails at dielectric constants below 15. In this region the curve increases monotonically.

Table IV. The Effect of Hydrogen Bonding on Buncel's Dye **1**

	absorption maximum[a]		
solvent	ethanol	methanol	water
experimental	550.1	543.2	548.2
uncorrected radii/with dispersion	504.3	499.7	506.9
uncorrected radii/without dispersion	431.0	431.2	433.5
corrected radii/with dispersion	539.8	532.9	543.3
corrected radii/without dispersion	435.4	435.2	438.1

[a] All values in nm.

The comparison between infinitely slow and infinitely fast relaxation is shown in Figures 2 and 3. Because the relaxation effect only influences the electrostatic component, there should be no large changes in the plot, which is dominated by the dispersion contribution. The fine structure of the electrostatic component is, however, lost and the curve is shifted by 5–10 nm to higher wavelengths.

Using the second (protic) solvent set we obtain the data shown in Table IV. It can be seen that hydrogen bonding lowers the absorption wavelengths by about 40 nm, although the fine structure for these three solvents is correct. We have tried to overcome the effect of hydrogen bonding in a simple, empirical way. We have adjusted the atomic van der Waals radii for these three solvents to reproduce the solvation energy of a set of 30 molecules.[58] These corrected values are shown in Table V. Using

(57) Buncel, E.; Rajagopal, S. *J. Org. Chem.* **1989**, *54*, 798.

Table V. Corrected Scaled van der Waals Radii for Consideration of the Effects of Hydrogen Bonding

	H	C	N	O
radius (Å)	1.42	1.96	1.55	1.50

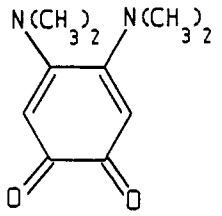

Figure 4. Structure of 4,5-bis(dimethylamino)-1,2-benzochinone (**2**).

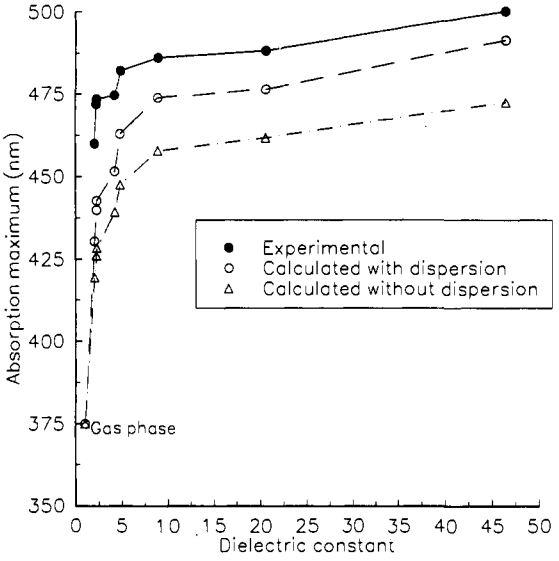

Figure 5. Solvent dependence of 4,5-bis(dimethylamino)-1,2-benzochinone (**2**) for the case of infinitely slow solvent reorientation.

this set of radii we can overcome the consistent error occurring in systems that show hydrogen-bonding effects. The results obtained are also shown in Table IV. The new radii do not correct the 40-nm error completely. This is clearly not the ideal way to overcome the deficiency of continuum models for hydrogen bonding, but it is more consistent with the model than a semicontinuum approach. The data given in Table IV also show the significant role of the dispersion contribution for this molecule.

In a second example we have calculated the solvatochromism of 4,5-bis(dimethylamino)-1,2-benzochinone (**2**) (shown in Figure 4), which has been investigated experimentally by Dähne and Seebacher.[59] The polarity dependence of this weak $\pi \rightarrow \pi^*$ absorption band is shown for the case of infinitely slow relaxation in Figure 5. In contrast to **1**, the dispersion contribution has much less influence on the fine structure of the curve obtained. There is only a nearly constant shift of about 15 nm. This shows that the dispersion contribution does not always dominate, but it is very important in some cases. The case of infinitely fast relaxation is shown in Figure 6. Here the fine structure in the region of small dielectric constants is lost again and at higher dielectric constants the calculated wavelengths are far higher than the absorption maxima.

C. Hypsochromic Solvent Shifts. We have also investigated a molecule that shows hypsochromic solvent shifts. The $\pi \rightarrow \pi^*$ absorption process of the 2,6-diphenyl-4-(2,4,6-triphenyl-1-pyridinio)phenoxide (**3**) of Reichardt[60] (normally abbreviated as $E_T(30)$, shown in Figure 7) is the best known in this class. The

(58) Rauhut, G. Ph.D. Thesis, University of Erlangen-Nürnberg, Germany, 1993.

(59) Dähne, S.; Seebacher, M. *Z. Chem.* **1972**, *12*, 141.

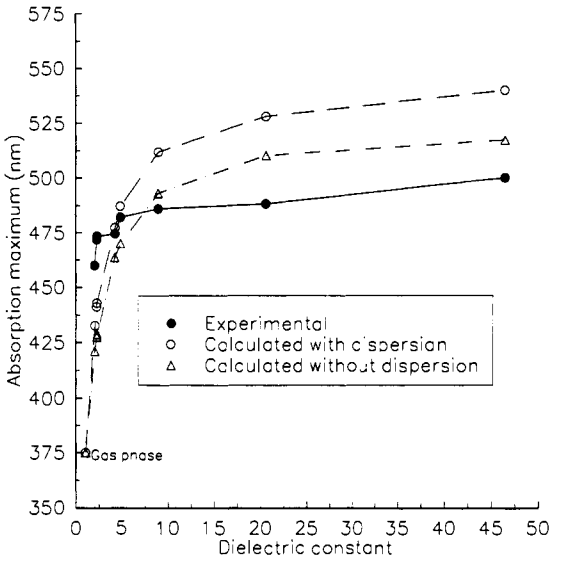

Figure 6. Solvent dependence of 4,5-bis(dimethylamino)-1,2-benzochinone (**2**) for the case of infinitely fast solvent reorientation.

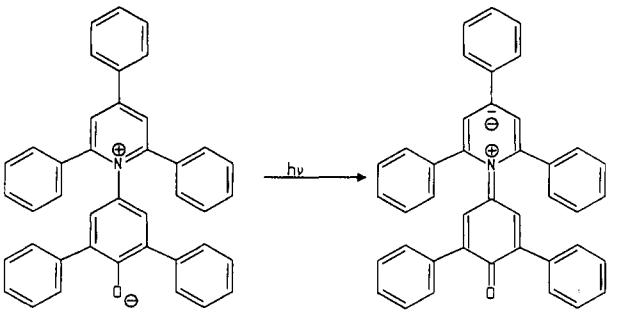

Figure 7. Excitation process of Reichardt's 2,6-diphenyl-4-(2,4,6-triphenyl-1-pyridinio)phenoxide (**3**).

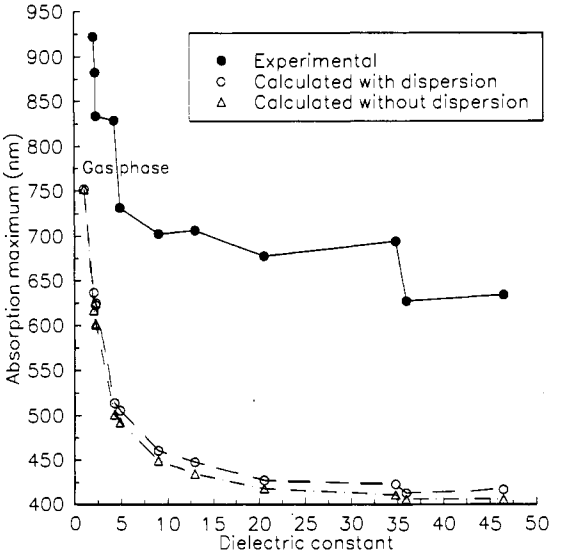

Figure 8. Solvent dependence of 2,6-diphenyl-4-(2,4,6-triphenyl-1-pyridinio)phenoxide (**3**) for the critical case of infinitely slow solvent reorientation.

solvent dependence of this absorption band for the case of infinitely slow relaxation is shown in Figure 8. The large gap between the experimental and the two calculated curves has two causes. Firstly,

(60) (a) Dimroth, K.; Reichardt, C.; Siepmann, T.; Bohlmann, F. *Liebigs Ann. Chem.* **1963**, *661*, 1. (b) Dimroth, K.; Reichardt, C. *Ibid.* **1969**, *727*, 93. (c) Reichardt, C. *Ibid.* **1971**, *752*, 64. (d) Reichardt, C. *Solvents and Solvent Effects in Organic Chemistry*; VCH: Weinheim, 1990; p 288.

small energetic changes in the region of about 700 nm cause large changes in the wavelength. Secondly, the weighting factor of 87% for the dispersion contribution for excited states (see above) was adjusted for bathochromic shifts. This may also be a reason for the weak dispersion effect obtained for this molecule. Nevertheless, the trend of the curve is well-represented. The calculated curve would show a much stronger fine structure if it were shifted into the region of the experimental one. Considering this effect, the energetic solvent shifts of the calculated curve are stronger than the experimental ones.

Conclusions

The numerical SCRF method presented above is capable of reproducing the experimental behavior of organic dyes in solution well. Considering that we have used our standard PECI = 8 configuration interaction expansion to calculate the excitation energies directly, both the absolute values of the absorption maxima and the shifts between different solvents are reproduced remarkably well. The major role of dispersion for some dyes is an important result. Clearly, large changes in polarizability between ground and excited states and large polarity changes make the dispersion contribution more important. Our limited experience suggests that dispersion is most important for extended systems which exhibit large bathochromic shifts, but more examples are needed.

One of the most important consequences of this work is that we should now be able to use SCRF theory to investigate the solvent effect on, for instance, the reorganization energy in electron-transfer reactions. The similarity between the excitation process in some solvatochromic dyes and intermolecular electron transfer suggests that we should obtain reliable results for such systems.

Possible improvements in the methodology given above include the use of charge-dependent atomic radii to describe the cavity and a more precise calculation of the free cavity energy. We hope that these improvements will allow us to approach experimental accuracy for solvation free energies.

Acknowledgment. This work was supported by the Deutsche Forschungsgemeinschaft, the Fonds der chemischen Industrie, the Volkwagenstiftung, and the Convex Computer GmbH. G.R. thanks the Studienstiftung des Deutschen Volkes for a fellowship and T.S. the Konrad-Zuse-Zentrum for support for visits to Erlangen.